Supporting Information

Ishibashi et al. 10.1073/pnas.1407888111

SI Materials and Methods

Cloning, Protein Expression, and Purification. Cloning of Tm-1(431) was performed as described in ref. 1. Tm-1(201)– and Tm-1(201/I91T)–encoding cDNAs were PCR amplified using the primers 5′-cacc*atcgaaggtagg*atggcaactgcacagagt-3′ (the Factor Xa cleavage site is italicized) and 5′-ctatcaactttcaagcctcccgatcaccat-3′ (the stop codon is underlined) and a plasmid encoding full-length Tm-1 or Tm-1(I91T) as the template and then were cloned individually into a pENTR/D-TOPO vector. The cDNA in each pENTR/D-TOPO vector was transferred into a pDEST-mal expression vector, and the proteins were expressed and purified as described (1). The helicase domain of the tomato mosaic virus (ToMV) replication proteins (ToMV-Hel) was cloned, expressed, and purified as described in ref. 2.

Preparation of the ToMV-Hel–Tm-1(431) Complex for Crystallization. Purified Tm-1 was dialyzed against 20 mM sodium phosphate (pH 7.5), 150 mM NaCl, 2 mM $MgCl_2$, 1 mM DTT and concentrated to ∼100 μM in an Amicon Ultra-15 30K system. Purified ToMV-Hel was mixed with Tm-1 and adenosine 5′-O-(3-thio) triphosphate (ATPγS) at a molar ratio of 1:1 and 1:10, respectively. The mixture was incubated at 4 °C for ∼1 h and then chromatographed through 200 pg HiLoad 26/60 Superdex (GE Healthcare Bio-Sciences) in 20 mM sodium phosphate (pH 7.5), 150 mM NaCl, 2 mM $MgCl_2$, 1 mM DTT, 0.1 mM ATP at 4 °C. The fractions containing the ToMV-Hel–Tm-1 complex were pooled and stored at 4 °C before crystallization.

Crystallization and Data Collection. Crystallization, data collection, and data processing for native and selenomethionine (SeMet)-labeled Tm-1(431) were performed as described in ref. 3. Briefly, SeMet-labeled Tm-1(431) and Tm-1(431) crystals were grown separately on siliconized coverslips by equilibrating a mixture containing 1.5 μL of the protein solution [10.0 mg protein·mL^{-1}, 20 mM Tris·HCl (pH 8.0), 50 mM NaCl, 1 mM DTT] and 1.5 μL of the reservoir solution [8.0% (wt/vol) PEG 8,000 and 0.4 M ammonium tartrate dibasic] against 400 μL of the reservoir solution. After crystal growth, each crystallization drop was equilibrated against reservoirs of increasing ethylene glycol concentration [5, 10, 15, and 20% (wt/vol)], and then the crystals were flash-frozen under a cryogenic stream of nitrogen gas. A three-wavelength multiwavelength anomalous diffraction (MAD) dataset for the SeMet–Tm-1(431) crystal was collected at the SPring-8 BL38B1 beamline at 100 K. The wavelengths in the MAD experiment were determined by a prior XAFS experiment that used a SeMet–Tm-1(431) crystal (Table S1). The datasets for SeMet–Tm-1(431) were processed using MOSFLM (4) and SCALA (5) as implemented in XIA2 (6). The datasets for Tm-1(431) were processed using the XDS/XSCALE (7) as implemented in XIA2 (6).

Tm-1(201/I91T) crystals were grown on a siliconized coverslip by equilibrating a mixture containing 1.5 μL of the Tm-1(201/I91T) solution [10.0 mg protein·mL^{-1} in 20 mM Tris·HCl (pH 8.0), 1 mM DTT] and 1.5 μL of the reservoir solution [4% (vol/vol) Tacsimate (Hampton Research), pH 6.0, and 12% (wt/vol) PEG 3,500] against 400 μL of the reservoir solution using the hanging-drop vapor-diffusion method at 20 °C. After crystal growth, the crystallization drop was serially equilibrated against reservoirs containing increasing concentrations of ethylene glycol [2.5, 5, 12.5, 20, and 25% (vol/vol)] with incubation times of 6–12 h. The crystal was flash-frozen in a cryogenic stream of nitrogen gas. A dataset was collected at the Photon Factory BL-5A beamline at 100 K.

ToMV-Hel–Tm-1(431) crystals were grown on a siliconized coverslip by equilibrating a mixture containing 1.5 μL of the ToMV-Hel–Tm-1(431) solution [5.0 mg of each protein·mL^{-1} in 20 mM sodium phosphate (pH 7.5), 150 mM NaCl, 2 mM β-mercaptoethanol, 0.4 mM ATPγS, 0.4 mM $MgCl_2$] and 1.5 μL of the reservoir solution [0.15 M CsCl, 15% (wt/vol) PEG 3,350] against 400 μL of the reservoir solution using the hanging-drop vapor diffusion method at 12 °C. The ToMV-Hel–Tm-1(431/I91T) crystals were grown on a siliconized coverslip by equilibrating a mixture containing 1.5 μL of the ToMV-Hel–Tm-1(431/I91T) solution [6.0 mg of each protein·mL^{-1} in 20 mM sodium phosphate (pH 7.5), 150 mM NaCl, 2 mM β-mercaptoethanol, 0.4 mM ATPγS, 0.4 mM $MgCl_2$, 66 μM $HgCl_2$] and 1.5 μL of the reservoir solution [0.2 M L-proline, 0.1 M Hepes·KOH (pH 7.0), 11% (wt/vol) PEG 3,350] against 400 μL of the reservoir solution. The ToMV-Hel–Tm-1(431) and ToMV-Hel–Tm-1(431/I91T) data were acquired at the SPing-8 BL38B1 and Photon Factory BL-17A beamlines at 100 K, respectively. The datasets for Tm-1(201/I91T), ToMV-Hel–Tm-1(431), and ToMV-Hel–Tm-1(431/I91T) were processed using the HKL2000 suite (8). The data collection and processing statistics are summarized in Table S1.

Structure Determination. MAD phasing, density modification, and initial model building for Tm-1(431) were performed using AutoSol and AutoBuild from the PHENIX program suite (9). Of the 60 possible selenium atoms in an asymmetric unit, 40 were found, and their positions were refined. A total of 1,456 residues were built into the electron density map automatically, and the side chain positions of 846 of these residues were fit into the electron density. The remaining parts of the molecule were constructed manually using COOT (10). The Tm-1(201/I91T) structure was determined by molecular replacement (MR) using MOLREP (11) and the coordinates of the Tm-1 NN-domains as the search model.

Attempts to solve the initial phases of the ToMV-Hel–Tm-1(431) complex by MR using the ToMV-Hel structure [Protein Data Bank (PDB) ID code 3VKW] (12) as a search model were unsuccessful. However, initial phases were obtained when the Tm-1(431) structure was used as the search model with MR by MOLREP (11), and the difference Fourier maps calculated from the complex's diffraction data using the Tm-1(431) model contained electron density associated with ToMV-Hel that could be used in conjunction with the free ToMV-Hel structure to build the remainder of the complex. The structure of ToMV-Hel–Tm-1(431/I91T) was determined using the coordinates of ToMV-Hel–Tm-1(431).

Refinements were followed by minimization with the crystallography and NMR system (CNS) (13) and iterative cycles of manual fitting. Then manual model building was carried out using COOT (10). The crystallographic models were refined using REFMAC (14) or CNS. Structural geometry was analyzed and validated by the MOLPROBITY (15). Phasing and refinement statistics are given in Table S1.

Inhibition of in Vitro ToMV RNA Replication. The assay protocol was essentially as described in refs. 16 and 17. To assess the activities of recombinant Tm-1 constructs, WT ToMV, *Tm-1* resistance-breaking ToMV mutant (LT1), or LT1(E979K) genomic RNA (800 ng) was individually translated in 100 μL of a membrane-depleted evacuolated BY-2 protoplast lysate-based translation mixture at 23 °C for 1 h. Then 14 μL of each translation mixture was mixed separately with 1 μL of 2.17 pmol of purified Tm-1(431), Tm-1(431/I91T), Tm-1(201), or Tm-1(201/I91T) in 20 mM Tris·HCl

(pH 8.0), 150 mM NaCl, 1 mM DTT or with buffer only and subsequently with 5 μL of the membrane preparation and was incubated at 15 °C for 1 h. For mutagenized Tm-$1^{PI126445}$ proteins (Fig. 5), WT ToMV RNA (40 ng in 5 μL of the translation mixture) and Tm-1 mRNA (1.38 μg in 10 μL of the translation mixture) synthesized by in vitro transcription using mScript mRNA production system reagents (Cellscript, Inc.) were individually translated at 23 °C for 1 h, mixed with each other, added into 5 μL of the membrane preparation, and incubated at 15 °C for 1 h. Then the substrates for RNA replication containing [α-^{32}P]CTP were added and further incubated at 23 °C for 1 h. ^{32}P-labeled RNA was purified by phenol extraction and ethanol precipitation, electrophoresed through a 2.4% (wt/vol) PAGE gel containing 8 M urea, and subjected to autoradiography. Band intensities were quantified using Multi Gauge v3.0 (Fujifilm).

Isothermal Titration Calorimetry for Characterizing Interactions Between Tm-1 and ToMV-Hel Constructs. To eliminate the heat of dilution effect, all protein solutions were dialyzed against 100 mM sodium phosphate (pH 7.5), 150 mM NaCl, 2 mM $MgCl_2$, 0.5 mM Tris(2-carboxyethyl)phosphine before calorimetry. Before each experiment, ATPγS (final concentration, 50 μM) was added into both protein solutions. Isothermal titration calorimetry (ITC) was carried out using a VP-ITC calorimeter (GE Healthcare Bio-Sciences) at 15 °C. The cell volume of the calorimeter was 1.4482 mL. Each Tm-1 solution (~150 μM) was taken up in a syringe for injection into the ToMV-Hel (~15 μM) solution. All samples were degassed before titration by centrifugation (14,000 × *g* for 30 min at 4 °C). The titrant was injected into the cell in 10-μL increments at 300-s intervals with stirring at 270 rpm. The titration data were processed with MicroCal Origin, Version 5.0.

ITC for Characterizing Interactions Between Tm-1(431/I91T) and ATP or GTP. Tm-1(431/I91T) protein was dialyzed against 100 mM sodium phosphate (pH 7.5), 150 mM NaCl, 2 mM $MgCl_2$, 0.5 mM Tris(2-carboxyethyl)phosphine before calorimetry. ITC was carried out using an iTC200 calorimeter (GE Healthcare Bio-Sciences) at 25 °C. The cell volume of the calorimeter was 0.2081 mL. ATP (1.44 mM) or GTP (1.67 mM) was dissolved in the same buffer as Tm-1(431/I91T), and the solutions were taken up in a syringe for injection into the Tm-1(431/I91T) solution (159 μM). All samples were degassed before titration by centrifugation (14,000 × *g* for 30 min at 4 °C). The titrant was injected into the reaction cell in 2-μL increments at 180-s intervals with stirring at 1,000 rpm. The titration data were processed with MicroCal Origin software, Version 5.0.

Measurement of the ToMV-Hel ATPase Activity by ITC. To eliminate the heat of dilution effect, all protein solutions used for calorimetry were dialyzed against 100 mM sodium phosphate (pH 7.5), 150 mM NaCl, 2 mM $MgCl_2$, 0.5 mM Tris(2-carboxyethyl) phosphine. ITC was carried out using a VP-ITC calorimeter (GE Healthcare Bio-Sciences) at 15 °C with stirring at 300 rpm. All samples were degassed before titration by centrifugation (14,000 × *g* for 30 min at 4 °C). The cell volume of the calorimeter was 1.4482 mL. A 100-μL solution of 3.8 μM ToMV-Hel or a mixture of 3.8 μM ToMV-Hel and Tm-1(431/I91T) was taken up in a syringe and injected 100 s after the 4.0-mM ATP solution had been added into the calorimetry cell over a period of 250 s. The titration data were processed with ITCenz (18).

Size-Exclusion Gel Chromatography. Purified ToMV-Hel was mixed with Tm-1(431) in the presence or absence of 2.0 mM ATP or with Tm-1(431/I91T) in the presence or absence of 2.0 mM ATP, ADP, or GTP. Each mixture was incubated at 4 °C for 2 h and then chromatographed through 200 pg HiLoad 10/300 GL Superdex (GE Healthcare Bio-Sciences) in 20 mM sodium phosphate (pH 7.5), 150 mM NaCl, 1 mM DTT, 2 mM $MgCl_2$ with or without 0.2 mM ATP, ADP, or GTP, as appropriate. The flow rate was 0.5 mL/min, and the temperature was 4 °C. Each peak fraction was subjected to SDS/PAGE. The separated proteins were visualized by Coomassie Brilliant Blue staining.

Molecular Dynamics Simulations. The crystallographic structure of ToMV-Hel–Tm-1(431) was used as the template for the LT1-Hel–Tm-1(431) and T21-Hel–Tm-1(431) complexes. The ToMV-Hel–Tm-1(431/I91T) complex was used as the template for the LT1-Hel–Tm-1(431/I91T), LT1(E979K)-Hel–Tm-1(431/I91T), and LT1(D1097Y)-Hel–Tm-1(431/I91T) complexes. The following protocol was applied to each of the complexes using MOE software (Chemical Computing Group, Inc.). For each complex, the rotamers of the mutated residue's angles were searched automatically by Rotamer Explorer, and the most appropriate set of angles for each mutated residue was selected after their values were examined manually. The protonate 3D protocol (19) in MOE was used to assign ionization states and hydrogen positions in the structures. Water molecules were added within 10 Å of I91 or T91 in Tm-1(431) or Tm-1(431/I91T), respectively. Because the complexes were very large, especially after water molecules had been added, and would have required long simulation times, only the residues within 10 Å of I91 or T91 were included in the simulations. Before the molecular dynamics (MD) simulations, the mutant structures were energy minimized to remove steric clashes. MD simulations were performed using the Amber12:EHT force field (Chemical Computing Group Inc.). A common MD protocol that heats the system from 0 to 300 K (100 ps) followed by equilibration, production for 500 ps, and cooling to 0 K (100 ps) was used.

1. Kato M, Ishibashi K, Kobayashi C, Ishikawa M, Katoh E (2013) Expression, purification, and functional characterization of an N-terminal fragment of the tomato mosaic virus resistance protein Tm-1. *Protein Expr Purif* 89(1):1–6.
2. Xiang H, et al. (2012) Expression, purification, and functional characterization of a stable helicase domain from a tomato mosaic virus replication protein. *Protein Expr Purif* 81(1):89–95.
3. Kato M, et al. (2013) Crystallization and preliminary X-ray crystallographic analysis of the inhibitory domain of the tomato mosaic virus resistance protein Tm-1. *Acta Crystallogr Sect F Struct Biol Cryst Commun* 69(Pt 12):1411–1414.
4. Powell HR (1999) The Rossmann Fourier autoindexing algorithm in MOSFLM. *Acta Crystallogr D Biol Crystallogr* 55(Pt 10):1690–1695.
5. Evans P (2006) Scaling and assessment of data quality. *Acta Crystallogr D Biol Crystallogr* 62(Pt 1):72–82.
6. Winter G (2010) xia2: an expert system for macromolecular crystallography data reduction. *J Appl Cryst* 43:186–190.
7. Kabsch W (1993) Automatic Processing of Rotation Diffraction Data from Crystals of Initially Unknown Symmetry and Cell Constants. *J Appl Cryst* 26:795–800.
8. Otwinowski Z, Minor W (1997) Processing of X-ray diffraction data collected in oscillation mode. *Methods Enzymol* 276:307–326.
9. Schneider TR, Sheldrick GM (2002) Substructure solution with SHELXD. *Acta Crystallogr D Biol Crystallogr* 58(Pt 10 Pt 2):1772–1779.
10. Emsley P, Cowtan K (2004) Coot: model-building tools for molecular graphics. *Acta Crystallogr D Biol Crystallogr* 60(Pt 12 Pt 1):2126–2132.
11. Lebedev AA, Vagin AA, Murshudov GN (2008) Model preparation in MOLREP and examples of model improvement using X-ray data. *Acta Crystallogr D Biol Crystallogr* 64(Pt 1):33–39.
12. Nishikiori M, et al. (2012) Crystal structure of the superfamily 1 helicase from Tomato mosaic virus. *J Virol* 86(14):7565–7576.
13. Brünger AT, et al. (1998) Crystallography & NMR system: A new software suite for macromolecular structure determination. *Acta Crystallogr D Biol Crystallogr* 54(Pt 5): 905–921.
14. Winn MD, Murshudov GN, Papiz MZ (2003) Macromolecular TLS refinement in REFMAC at moderate resolutions. *Macromolecular Crystallography* 374(Pt D): 300–321.
15. Davis IW, et al. (2007) MolProbity: all-atom contacts and structure validation for proteins and nucleic acids. *Nucleic Acids Res* 35(Web Server issue):W375–383.
16. Ishibashi K, Komoda K, Ishikawa M (2006) In vitro translation and replication of Tobamovirus RNA in a cell-free extract of evacuolated tobacco BY-2 protoplasts. *Tobacco BY-2 Cells* (Springer, Berlin).
17. Ishibashi K, Naito S, Meshi T, Ishikawa M (2009) An inhibitory interaction between viral and cellular proteins underlies the resistance of tomato to nonadapted tobamoviruses. *Proc Natl Acad Sci USA* 106(21):8778–8783.

18. Karim N, Kidokoro S (2004) Precise and continuous observation of cellulase-catalyzed hydrolysis of cello-oligosaccharides using isothermal titration calorimetry. *Thermochim Acta* 412(1-2):91–96.

19. Labute P (2009) Protonate3D: assignment of ionization states and hydrogen coordinates to macromolecular structures. *Proteins* 75(1):187–205.

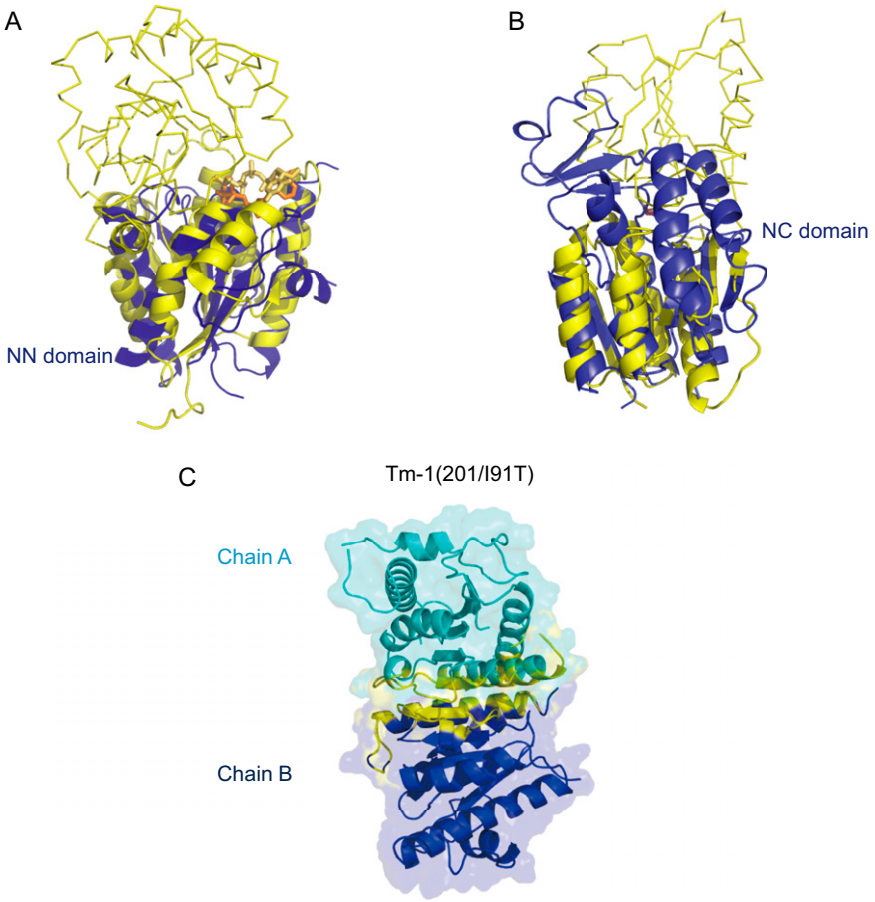

Fig. S1. Structural comparison of the NN and NC domains of Tm-1 and similar proteins. (*A*) Ribbon diagrams showing the superposition of the Tm-1(431) NN domain (blue) and the N-terminal domain of the nonhydrolyzing bacterial UDP-GlcNAc 2-epimerase (PDB ID code 3BEO; yellow). The superpositioned proteins have a *Z* score of 11.0 and a Cα rmsd value of 3.6 Å as calculated at the distance alignment matrix method (DALI) server (1). ATPγS is shown as an orange stick model at the binding cavity found in the ToMV-Hel–Tm-1(431) complex (Fig. 3*C*). Note that the Tm-1 residues that interact with ATPγS correspond to those of the UDP-GlcNAc binding site (represented as a yellow stick model) in UDP-GlcNAc 2-epimerase. (*B*) Ribbon diagrams showing the superposition of the Tm-1(431) NC domain (blue) with the N-terminal domain of the *Thermotoga maritime* ribose-binding protein (PDB ID code 2FN8; yellow). The superpositioned proteins have a Z score of 9.4 and a Cα rmsd value of 3.0 Å as calculated at the DALI server. (*C*) Crystal structure of Tm-1(201/I91T). The polypeptide chains that form the dimer are colored blue or cyan. The buried surface area of the dimer interface is ∼3,400 $Å^2$ as calculated by Protein Interfaces, Surfaces and Assemblies (PISA) (2). The dimer interface is formed mainly by an extensive set of hydrophobic interactions and hydrogen bonds between β5–β5 and α6–α6, shown in yellow (Tables S2 and S3).

1. Holm L, Rosenström P (2010) Dali server: Conservation mapping in 3D. *Nucleic Acids Res* 38(Web Server issue):W545-9.
2. Krissinel E, Henrick K (2007) Inference of macromolecular assemblies from crystalline state. *J Mol Biol* 372(3):774–797.

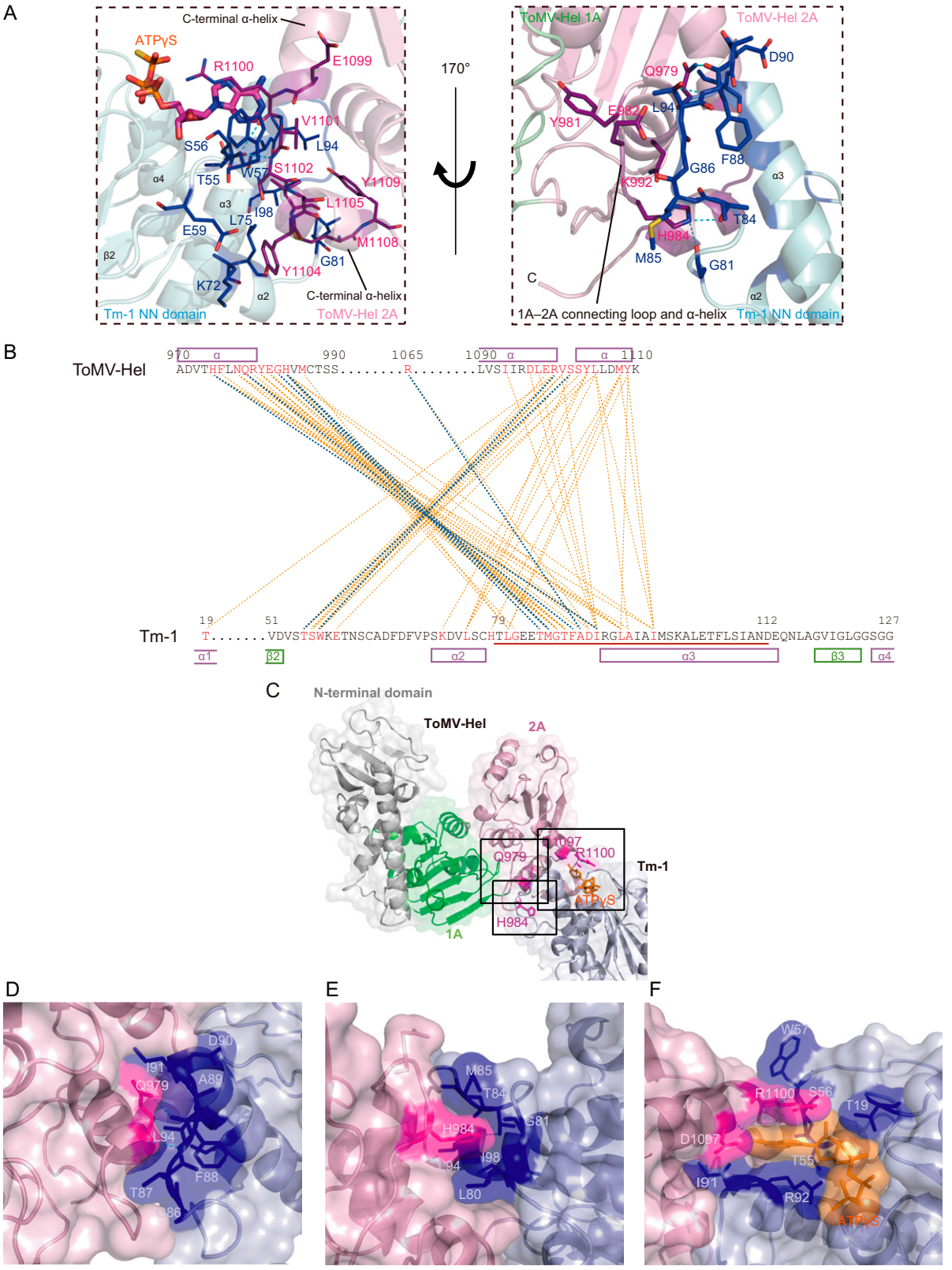

Fig. S2. Close-up view of the ToMV-Hel–Tm-1(431) interface and ToMV-Hel residues important for escaping Tm-1 inhibition. (*A*) Close-up view of the ToMV-Hel–Tm-1(431) interface before (*Left*) and after (*Right*) a 170° rotation around the vertical axis. The Tm-1 polypeptide chains are colored blue, and those of the ToMV-Hel 2A domain are colored pink. Interacting residues of Tm-1(431) and ToMV-Hel are shown as blue and violet stick models, respectively. ATPγS is represented as a stick model with oxygen atoms in red, nitrogen atoms in blue, sulfur atoms in yellow, phosphorous atoms in orange, and carbon atoms in magenta. (*B*) Map of interacting Tm-1(431) and ToMV-Hel residues. The hydrogen bonds and the van der Waals contacts between the residues are shown as cyan and orange dotted lines, respectively. (*C*) Close-up view showing the ToMV-Hel residues in the ToMV-Hel–Tm-1(431) complex that, when mutated, allow

Legend continued on following page

ToMV-Hel to escape inhibition by Tm-1. The N-terminal domain and domains 1A and 2A of ToMV-Hel are colored gray, green, and magenta, respectively. (*D*) Close-up view of ToMV-Hel Q979 at the ToMV-Hel–Tm-1(431) interface. (*E*) Close-up view of ToMV-Hel H984 at the ToMV-Hel–Tm-1(431) interface. (*F*) Close-up view of ToMV-Hel D1097 and R1100 at the ToMV-Hel–Tm-1(431) interface. In *D*, *E*, and *F*, ToMV-Hel Q979, H984, D1097, and R1100 are shown as magenta stick models; Tm-1 residues that interact with Q979, H984, D1097, and/or R1100 are shown as blue stick models; and ATPγS is shown as an orange stick model.

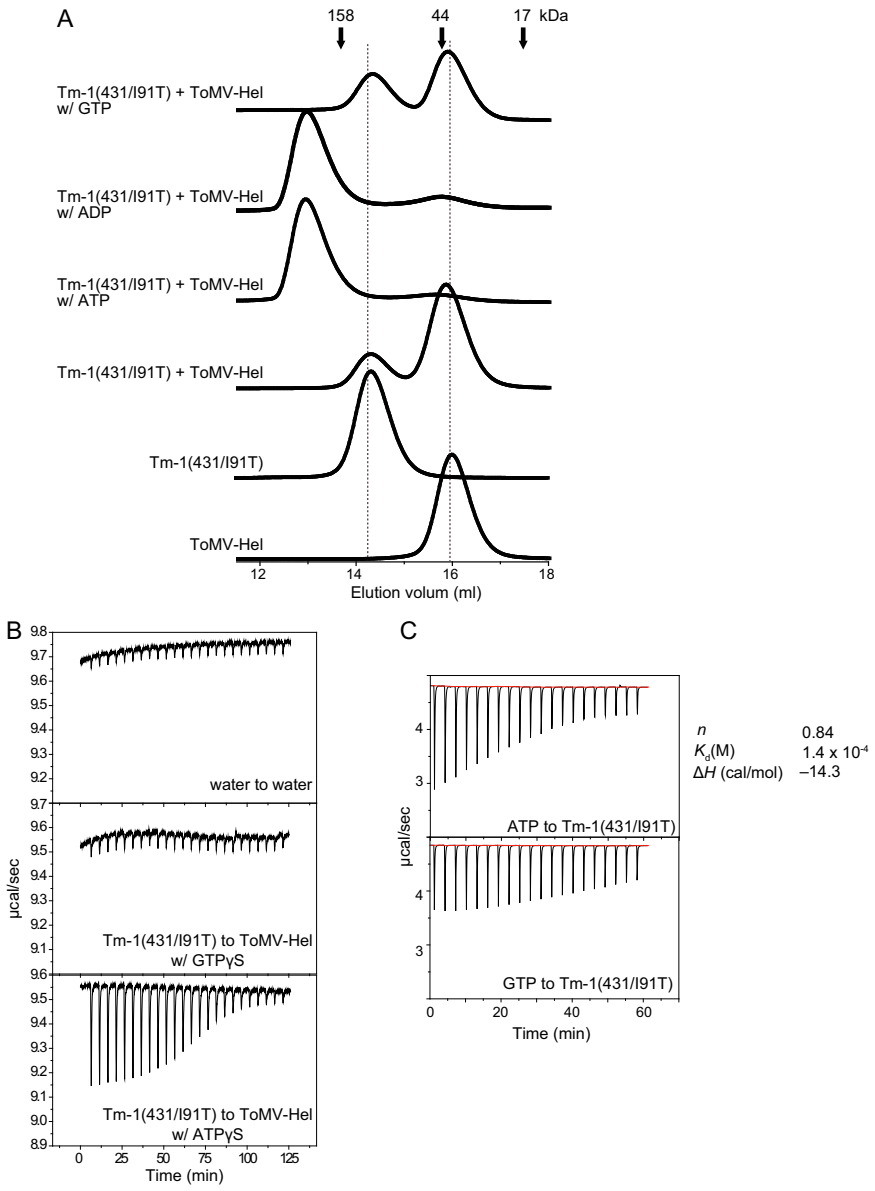

Fig. S3. ATP and ADP, but not GTP, support the association of Tm-1(431) and ToMV-Hel. (*A*) Size-exclusion gel chromatographs of ToMV-Hel and Tm-1(431/I91T) in the presence and absence of ATP, ADP, or GTP. Chromatography was performed as described for the results of Fig. 2*A*. (*B*, *Top*) ITC control (no protein present). (*Middle*) ITC titration showing the interaction between ToMV-Hel and Tm-1(431/I91T) when 2 mM GTPγS is present. (*Bottom*) ITC titration showing the interaction between ToMV-Hel and Tm-1(431/I91T) when 2 mM ATPγS is present. (*C*) ITC showing the interactions between Tm-1(431/I91T) and ATP (*Upper*) or GTP (*Lower*).

Table S1. X-ray diffraction data and crystal structure refinement statistics

	Tm-1(431)			Tm-1(201/I91T)	ToMV-Hel–Tm-1(431)	ToMV-Hel–Tm-1(431/I91T)
Data collection		SeMet		Native	Native	Native
Wavelength, Å	Peak: 0.9788	Edge: 0.9792	Remote: 0.9639	1.0000	1.0000	1.0000
Temperature, K		100		100	100	100
Space group		*P*1		$P2_12_12_1$	$P2_12_12_1$	$P2_12_12_1$
Unit cell parameters						
a, *b*, *c*, Å		77.97, 105.28, 110.62		74.57, 101.40, 46.93	82.22, 133.71, 195.22	84.98, 133.55, 195.79
α, β, γ, °		94.6, 109.3, 108.0				
Resolution, Å*	49.54–2.89 (3.04–2.89)	49.52–2.90 (3.06–2.90)	49.63–2.71 (2.86–2.71)	41.96–2.75 (2.80–2.75)	46.31–2.50 (2.54–2.50)	33.75–2.30 (2.34–2.30)
Reflections						
Unique	62,196 (8,104)	54,549 (7,433)	79,784 (11,683)	9,706 (499)	77,701 (3833)	99,309 (4,806)
Completeness, %	90.4 (80.4)	80.1 (74.7)	95.0 (95.5)	95.3 (97.5)	99.4 (99.4)	99.6 (98.5)
Redundancy	7.8 (7.8)	7.8 (7.8)	2.0 (2.0)	4.3 (4.2)	6.9 (6.7)	3.9 (3.8)
I, σ(I)	12.3 (3.1)	12.8 (3.3)	10.2 (3.1)	15.6 (2.6)	19.6 (3.5)	25.2 (3.2)
R_{sym} I†, %	4.9 (24.5)	4.7 (23.1)	5.7 (23.7)	10.2 (27.3)	9.5 (39.2)	5.3 (39.2)
Refinement			Refmac	Refmac	CNS	CNS
Resolution, Å			49.64–2.71	41.96–2.75	46.31–2.50	33.75–2.30
Reflections, work/test			72,019/3,790	8,811/442	75,084/3,800	9,4449/4,771
R_{work}/R_{free}, %			21.1/27.8	19.1/24.6	19.6/24.0	20.2/24.8
Number of molecules						
Water			44	7	778	739
Ligands			2 (TLA)	0	4 (ATPγS) 3 (Mg^{2+}) 18 (CS^{+})	4 (ATPγS) 4 (Mg^{2+}) 1 (Cl^{-})
Average B-factors			67.9	55.8	32.9	49.5
Rmsd						
Bond lengths, Å			0.012	0.011	0.006	0.006
Bond angles, °			1.5	1.5	1.2	1.2
Ramachandran (no. residues/%)						
Allowed			2,245/96.4	340/96.3	1,579/93.9	1,683/99.5
Favored			1,926/82.7	318/90.1	1,668/99.2	1,603/94.8
Disallowed			85/3.64	13/3.68	13/0.8	8/0.5

Values in intensity statistics for Tm-1(431) refer to our previous report (3). TLA, tartaric acid.
*Data for each of the highest-resolution shells are given in parentheses.
†$R_{sym}(I) = \Sigma_{hkl}\Sigma_i|I_i(hkl) - \langle I(hkl)\rangle|/\Sigma_{hkl}\Sigma_i|I_i(hkl)|$; for *n* independent reflections and *i* observations of a given reflection; <I(hkl)>, average intensity of the *i*th observation.

Table S2. Hydrogen bonds formed between atoms of Tm-1(431) chains A and B* found by PISA

Chain A		Chain B	
Residue (atom)	Location	Residue (atom)	Location
Gly141 (O)	Loop linking α4 and β4 (NN)	Ans186 (ND2)	α6 (NN)
Ala151 (O)	Loop linking β4 and β5 (NN)	Thr155 (OG1)	Loop linking β4 and β5 (NN)
Ser152 (OG)	Loop linking β4 and β5 (NN)	Gly160 (N)	Loop linking β4 and β5 (NN)
Ser152 (OG)	Loop linking β4 and β5 (NN)	Gly160 (O)	Loop linking β4 and β5 (NN)
Gly153 (N)	Loop linking β4 and β5 (NN)	Thr155 (OG1)	Loop linking β4 and β5 (NN)
Gly153 (O)	Loop linking β4 and β5 (NN)	Thr155 (N)	Loop linking β4 and β5 (NN)
Gly153 (O)	Loop linking β4 and β5 (NN)	Thr155 (OG1)	Loop linking β4 and β5 (NN)
Gln154 (N)	Loop linking β4 and β5 (NN)	Gln154 (OE1)	Loop linking β4 and β5 (NN)
Gln154 (OE1)	Loop linking β4 and β5 (NN)	Gln154 (N)	Loop linking β4 and β5 (NN)
Thr155 (N)	Loop linking β4 and β5 (NN)	Gly153 (O)	Loop linking β4 and β5 (NN)
Gly160 (N)	Loop linking β4 and β5 (NN)	Ser152 (OG)	Loop linking β4 and β5 (NN)
Gly160 (O)	Loop linking β4 and β5 (NN)	Ser152 (OG)	Loop linking β4 and β5 (NN)
Asn178 (ND2)	α6 (NN)	Phr261 (O)	Loop linking α2 and β3 (NN)
Asn178 (OD1)	α6 (NN)	Thr213 (OG1)	β1 (NC)
Asn186 (ND2)	α6 (NN)	Gly141 (O)	Loop linking α4 and β4 (NN)
Lys230 (NZ)	α2 (NC)	Cys174 (SG)	α4 (NN)

*Chains A and B identify the two monomers in the Tm-1 dimer. NC and NN indicate the NC domain (residues 211–431) and the NN domain (residues 1–201) of Tm-1(431), respectively.

Table S3. van der Waals contacts between residues of Tm-1(431) chains A and B* found by PISA

Location	Residue	
	Chain A	Chain B
α1 (NN)	Ser37	Phe38, Asn40, Glu200
	Phe38	Ser37, Phe38, Gly193, Ile196, Gly197
Loop linking α3 and β3 (NN)	Ile140	Val170, Val182, Val183
	Gly141	Val182, N186
	Pro143	N186
Loop linking β4 and β5 (NN)	Ala151	Thr155, Ile159
	Ser152	Thr155, E156, Ile159, G160, Thr161
	Gly153	Gly153, Gln154, Thr155, Glu156
	Gln154	Gly153, Gln154, Thr155
	Thr155	Ala151, Ser152, Gly153, Gln154, Thr155
	Ile159	Ala151, Ser152, P168
	Gly160	Ser152
	Thr161	Ser152, Val170
	Ser162	Pro168, Val170
	Asp163	Pro168, Val170, Val183, Asn186
	Leu164	Pro168
	Val165	Val165, Leu166, Phe167, Pro168
β5 (NN)	Leu166	Val165, Leu166
	Phe167	Val165, Phe167, Met194
	Pro168	Ile159, Ser162, Asp163, Leu164, Val-165
Loop linking β5 and α6 (NN)	Val170	Thr161, Ser162, Asp163
	Val171	Leu241, Phe243, Leu256
	Asn177	Leu241, Leu256, Phe261
	Asn178	Glu239, Leu241
α6 (NN)	Val179	Glu239, Phe261, Gln262
	Val182	Ile140, Phe261
	Val183	Asp163
	Asn186	Gly141, Ile142, Pro143, Asp163, Met194, Arg198
	Ala189	Ala190, Gly193, Met194, Gly197
	Ala190	Ala189, Ala190, Gly193, Met194
	Gly193	Ala189, Ala190, Gly193
	Met194	Phe167, Asn186, Ala189, Ala190
	Ile196	Phe38
	Gly197	Leu241, Leu256, Phe261
β2 (NC)	Glu239	Phe38
	Leu241	Ile176, Asn177, Asn178
	Val242	Val171, Asn177, Asn178, Val-179
	Phe243	Asp172
	Ala252	Val171
	Leu256	Val170

*Chains A and B identify the two monomers in the Tm-1 dimer.

Table S4. Hydrogen bonds formed by atoms of Tm-1(431) or Tm-1(431/I91T) and those of ToMV-Hel found by PISA

ToMV-Hel–Tm-1(431)			ToMV-Hel–Tm-1(431/I91T)		
Residue (atom)			Residue (atom)		
Tm-1(431)	ToMV-Hel	Distance, Å	Tm-1(431/I91T)	ToMV-Hel	Distance, Å
Thr55 (O)	Ser1102 (N)	2.86	Thr55 (O)	Ser1102 (N)	2.79
Trp57 (N)	Arg1100 (O)	3.11	Trp57 (N)	Arg1100 (O)	2.96
Thr84 (OG1)	His984 (NE2)	2.64	Gly81 (O)	His984 (NE2)	2.94
Met85 (O)	Gly983 (N)	2.64	Met85 (O)	Gly983 (N)	2.68
Met85 (O)	His984 (N)	2.62	Phe88 (O)	Arg1065 (NH2)	3.05
Phe88 (O)	Gln979 (NE2)	3.81	Phe88 (N)	Gln979 (O)	3.02
Phe88 (N)	Gln979 (O)	2.92	Thr91 (O)	His975 (NH2)	3.0
Ala89 (O)	Arg1065 (NH1)	2.97	Thr91 (OG1)	Gln979 (NE2)	2.80
Ile91 (O)	His975 (NE2)	3.10			

Table S5. van der Waals contacts between residues of chain A in Tm-1(431) or Tm-1(431/I91T) and those of ToMV-Hel found by PISA

ToMV-Hel–Tm-1(431)		ToMV-Hel–Tm-1(431/I91T)	
Tm-1(431)	ToMV-Hel	Tm-1(431/I91T)	ToMV-Hel
Thr19	Arg1100	Thr19	Arg1100
Thr55	Arg1100, Val1101, Ser1102, Leu1105	Thr55	Arg1100, Val1101, Ser1102, Leu1105
Ser56	Arg1100, Val1101, Ser1102	Ser56	Arg1100, Val1101, Ser1102
Trp57	Glu1099, Arg1100, Val1101, Ser1102, Ser1103	Trp57	Lys993, Glu1099, Arg1100, Val1101, Ser1102, Ser1103
Glu59	Tyr1104	Glu59	Tyr1104
Lys72	Tyr1104	Lys72	Tyr1104
Leu75	Ser1102, Tyr1104, Leu1105, Met1108	Leu75	Ser1102, Tyr1104, Leu1105, Met1108
His78	Met1108	His78	Met1108
Leu80	His984, Met986, Met1108, Tyr1109	Leu80	His984, Met986, Met1108, Tyr1109
Gly81	His984	Gly81	His984
Thr84	His984	Thr84	His984
Met85	Tyr981, Glu982, Gly983, His984	Met85	Asn978, Tyr981, Glu982, Gly983, His984
Gly86	Asn978, Gln979, Tyr981, Glu982, Gly983	Gly86	Asn978, Gln979, Tyr981, Glu982, Gly983
Thr87	Asn978, Gln979, Arg980, Tyr981, Glu982	Thr87	Asn978, Gln979, Arg980, Tyr981, Glu982
Phe88	Gln979	Phe88	Asn978, Gln979
Ala89	Gln979, Arg1065	Ala89	Gln979, Arg1065
Asp90	Gln979, Arg1065	Asp90	Gln979, Arg1065, Asp1097
Ile91	His975, Phe976, Gln979, Ile1094, Asp1097, Leu1098, Val1101	Thr91	His975, Gln979, Ile1094, Asp1097, Leu1098, Val1101
Leu94	His975, Asn978, Gln979, His984, Tyr1109	Leu94	His975, Asn978, Gln979, Tyr1109
Ala95	His975, Leu1105	Ala95	His975, Val1101, Leu1105
Ile98	His975, His984, Leu1105, Met1108, Tyr1109	Ile98	His975, Leu1105, Met1108, Tyr1109

Table S6. Hydrogen bonds formed between atoms of ATPγS and Tm-1(431), Tm-1(431/I91T), or ToMV-Hel in ToMV-Hel–Tm-1(431) or ToMV-Hel–Tm-1(431/I91T) found by LIGPLOT*

ToMV-Hel–Tm-1(431)				ToMV-Hel–Tm-1(431/I91T)			
	Residue (atom)	ATPγS, atom	Distance, Å		Residue (atom)	ATPγS, atom	Distance, Å
Tm-1(431)	Thr55 (OG1)	N3	2.71	Tm-1(431/I91T)	Thr55 (OG1)	N3	2.86
	Ser125 (OG)	O2G	2.73		Arg92 (NH1)	O2G	3.16
	Arg92 (NH1)	O2G	3.23		Arg92 (NH2)	O2G	2.83
	Gly124 (N)	O1B	2.99		Gly127 (N)	O1B	3.03
	Gly127 (N)	O1B	2.94		Gly124 (N)	O1B	2.85
	Lys20 (NZ)	O2B	2.84		Lys20 (NZ)	O2B	2.61
	Gly126 (N)	O3B	2.87		Gly126 (N)	O3B	2.98
	Lys20 (NZ)	O1A	2.82		Lys20 (NZ)	O1A	2.76
	Arg92 (NH2)	O3G	2.72		Thr19 (OG1)	O1A	2.89
					Thr55 (N)	O3	3.17
ToMV-Hel	Asp1097 (OD1)	N6	3.32	ToMV-Hel	Asp1097 (O)	N6	2.97
	Asp1097 (O)	N6	3.13		Arg1100 (NH2)	O2	3.23

*Available at www.ebi.ac.uk/thornton-srv/software/LIGPLOT/.